Supplementary Information

Non-stick performance of polymethylsilsesquioxane thin films synthesized by sol-gel spray coating

Toshiyuki Kajioka,*[a] Koji Ikegami[a] and Hiromitsu Kozuka[b]

[a] Nippon Electric Glass Co., Ltd., Nagahama, Shiga, Japan

[b] Department of Chemistry and Materials Engineering, Kansai University, Suita, Japan

***Correspondence author:** Toshiyuki Kajioka (tkajioka@neg.co.jp)

S.1. Materials used for the coating solutions

Methyltrimethoxysilane (MTMS), tetraethyl orthosilicate (TEOS), and trimethylchlorosilane (TMCS) were purchased from Tokyo Chemical Industry Co. Ltd. Isopropyl alcohol (IPA) was purchased from Sasaki Chemical Co. Ltd. Aqueous hydrochloric acid (HCl) and aqueous ammonia (NH_3) were purchased from Fujifilm Wako Pure Chemical Corporation. Deionized water with a minimum resistivity of 18 MΩcm was used.

S.2. Hydrolytic stability of hydrophobic coatings formed with mono-functional silanes

First, a mixture was prepared with a TEOS:TMCS:IPA:H_2O molar ratio of 0.8:0.2:4:4. Herein, a solution of TEOS and TMCS was mixed with a solution of IPA and H_2O. Then, hydrolysis and condensation reactions were performed at 45 °C for 4 h. Finally, the solution was diluted with IPA to an amount corresponding to a molar ratio of IPA/(TEOS + TMCS) = 102. The spray conditions were the same as those used to prepare A0G–A3G and B1G. After spray coating, the film was heated at 350 °C for 30 min. The water contact angle (WCA) of the resulting film was 84.6°. After immersion in boiling water for 1 h, the WCA decreased to 33.2°. After boiling, the sample was subsequently heated at 250 °C for 30 min; however, the WCA remained low at 34.9°. The initial high WCA of this coating was achieved due to the presence of monofunctional trimethylsilyl groups (-Si(CH_3)$_3$); however, these groups were likely cleaved via hydrolysis during boiling (Si-O-Si(CH_3)$_3$ + H_2O → Si-OH + HO-Si(CH_3)$_3$).

S.3. Effect of surface roughness on hydrophobicity and non-stick performance

The PMSQ surfaces in this study were slightly rough, as shown in the images in Figure S1. This morphology may be due to the formation of a "rim-lamella" structure upon droplet impact on the substrate during spraying, as described in our previous research on anti-glare coatings.[S1,S2]

Table S1 lists the surface roughness values obtained using a white-light interferometric microscope (NewView7300, Zygo). The roughness parameters included the root mean square height (Sq), root mean square gradient (Sdq), and developed interfacial area ratio (Sdr). All the samples exhibited very low Sdr values. That is, the surface area enhancement due to roughening was very small, suggesting that the impact of the Wenzel effect[S3] on the WCA was negligible.

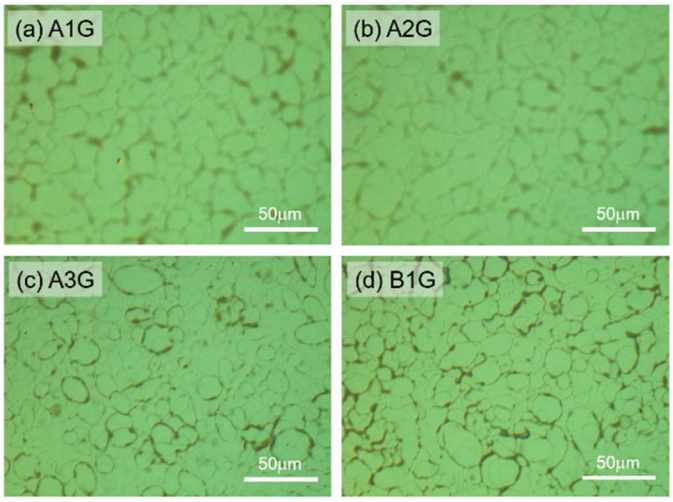

Figure S1 Surface images captured using a differential interference contrast microscope: (a) A1G, (b) A2G, (c) A3G and (d) B1G.

Table S1 Film thickness and roughness values (mean ± standard error) obtained using a white-light interferometric microscope.

Sample	Film thickness (nm)	Roughness values		
		Sq (nm)	Sdq	Sdr (%)
Non-coated N-0	-	0.6 ±0.0	0.002 ± 0.000	0.000 ± 0.000
A1G	16.8 ± 1.0	8.4 ± 0.2	0.006 ± 0.000	0.001 ± 0.000
A2G	15.2 ± 1.1	7.3 ± 0.2	0.006 ± 0.000	0.002 ± 0.000
A3G	16.1 ± 0.7	11.2 ± 0.2	0.014 ± 0.000	0.010 ± 0.000
B1G	16.5 ± 1.3	17.4 ± 0.3	0.019 ±0.000	0.019 ± 0.001

To observe with higher lateral resolution, field emission scanning electron microscopy (FE-SEM; SU8200, Hitachi) was employed. Figure S2 shows the FE-SEM images, which reveal a significantly smooth surface.

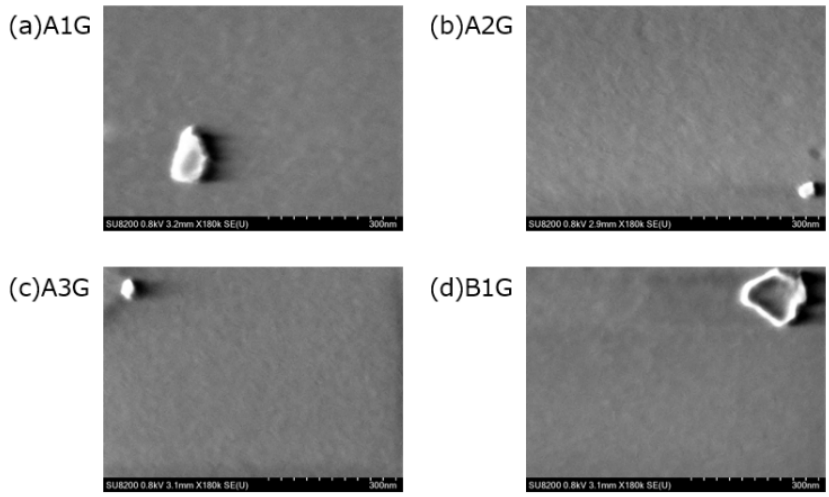

Figure S2 FE-SEM images of (a) A1G, (b) A2G, (c) A3G, and (d) B1G. An image including dust was captured to verify the focus. Although charge accumulation resulted in image distortion around the dust particles, the remaining surface maintained a smooth appearance.

To further investigate the effect of surface roughness, sample A2G' was prepared by coating sol A2 onto an N-0 plate with a rough surface. The N-0 plate with a rough surface was fabricated by forming a rough SiO_2 layer as described in the following paragraph. Table S2 lists the resultant WCA, non-stick properties, and roughness values. Although A2G' exhibited increased surface roughness as compared to A2G, its WCA and non-stick performance remained similar and did not reach the level of A3G.

Table S2 WCAs, non-stick performance, and roughness values of bare N-0, N-0 with a rough silica layer, A2G, and A2G' (mean ± standard error). The surface roughness values were measured using a white-light interferometric microscope.

Sample	Sol for non-stick coating	WCA (°)	Area fraction of burnt-on residue (%) (Barbecue sauce)	Roughness values		
				Sq (nm)	Sdq	Sdr (%)
Non-coated N-0	-	4.3 ± 0.2	96.0 ± 0.3	0.6±0.0	0.002±0.000	0.000±0.000
N-0 with a rough SiO_2 layer	-	15.1 ± 0.1	97.1 ± 0.6	8.3±0.3	0.016±0.000	0.012±0.001
A2G	A2	94.8 ± 0.1	5.4 ± 0.9	7.3±0.2	0.006±0.000	0.002±0.000
A2G'	A2	94.5 ± 0.2	6.0 ± 0.5	11.6±0.2	0.020±0.001	0.017±0.002

The rough SiO_2 layer was formed on the N-0 surface as follows, using a method similar to the silica sol spray technique for anti-glare coatings.[S1,S2] TEOS, IPA, HCl, and H_2O were mixed in a molar ratio of 1:2:0.02:7. First, TEOS was mixed with half the amount of IPA, and HCl and H_2O were mixed with the remaining IPA. The latter mixture was then added to the former. After mixing, hydrolysis and condensation reactions were performed at 45 °C for 4 h. The resulting solution was diluted with IPA to achieve a final molar ratio of 92:1 relative to the initially used TEOS. Spray coating was performed with a pitch of 4 mm under the same conditions as those used for A0G–A3G and B1G. After spraying, the sample was heated at 350 °C for 30 min.

Based on these results, the differences in the WCA and non-stick performance among the samples were attributed to surface chemistry rather than surface morphology.

S.4. Dynamic contact angles and surface free energies

Table S3 Static (θ_s), advancing (θ_a), and receding (θ_r) contact angles of water and n-hexadecane (mean ± standard error), together with the calculated contact angle hysteresis and surface free energy (γ). γ_p and γ_d represent the polar and dispersive components of the surface free energy, respectively.

	Water				n-Hexadecane				
Sample	θ_s (°)	θ_a (°)	θ_r (°)	$\theta_a - \theta_r$ (°)	θ_s (°)	θ_a (°)	θ_r (°)	$\theta_a - \theta_r$ (°)	γ (mN·m^{-1})
A0G	84.4 ± 0.2	91.4 ± 0.7	77.9 ± 0.1	13.5	35.3 ± 0.3	37.7 ± 0.3	34.3 ± 0.5	3.4	28.9 [γ_p 6.1, γ_d 22.8]
A1G	90.5 ± 0.2	98.9 ± 0.2	85.1 ± 0.5	13.8	33.3 ± 0.2	35.5 ± 0.4	32.6 ± 0.3	2.9	26.9 [γ_p 3.6, γ_d 23.3]
A2G	94.8 ± 0.1	102.6 ± 0.3	87.4 ± 0.4	15.2	31.3 ± 0.2	33.9 ± 0.3	28.7 ± 0.7	5.2	25.9 [γ_p 2.2, γ_d 23.7]
A3G	97.4 ± 0.2	103.8 ± 0.4	88.5 ± 0.4	15.3	30.9 ± 0.2	34.0 ± 0.7	29.4 ± 0.6	4.6	25.4 [γ_p 1.6, γ_d 23.8]
B1G	93.5 ± 0.3	99.9 ± 0.2	86.8 ± 0.1	13.1	33.1 ± 0.2	35.6 ± 0.1	31.4 ± 0.3	4.2	26.0 [γ_p 2.7, γ_d 23.3]

Table S3 lists the dynamic contact angles and surface free energy values. The advancing and receding contact angles were measured by the extension-contraction method using a contact angle meter (DMs-401, Kyowa Interface Science Co., Ltd.), and the surface free energies were calculated using the Owens-Wendt-Rabel-Kaelble method.[S4] Here, the polar and dispersive components of the surface tension were taken as 51.0 and 21.8 mN·m^{-1} for water, and 0 and 27.6 mN·m^{-1} for n-hexadecane, respectively. There were only slight differences in contact angle hysteresis among the samples. A3G exhibited the lowest surface free energy, particularly in the polar component. This is attributed to the increased presence of Si–CH_3 groups on the surface.

References (Supplementary Information)

S1 T. Kajioka, T. Kanai, K. Ikegami and H. Kozuka, *J. Sol-Gel Sci. Technol*., 2021, **100**, 244–251. DOI: 10.1007/s10971-021-05664-1.
S2 T. Kajioka, T. Kanai, K. Ikegami and H. Kozuka, *Int. J. Appl. Glass Sci.*, 2025, **16**, 16692. DOI: 10.1111/ijag.16692.
S3 R. N. Wenzel, *Ind. Eng. Chem*., 1936, **28**, 988–994. DOI: 10.1021/ie50320a024.
S4 D. K. Owens and R. C. Wendt, *J. Appl. Polym. Sci.*, 1969, **13**, 1741-1747. DOI: 10.1002/app.1969.070130815.